We are IntechOpen,
the world's leading publisher of Open Access books
Built by scientists, for scientists

4,800
Open access books available

122,000
International authors and editors

135M
Downloads

154
Countries delivered to

Our authors are among the

TOP 1%
most cited scientists

12.2%
Contributors from top 500 universities

BOOK CITATION INDEX
CLARIVATE ANALYTICS
INDEXED

WEB OF SCIENCE™

Selection of our books indexed in the Book Citation Index
in Web of Science™ Core Collection (BKCI)

Interested in publishing with us?
Contact book.department@intechopen.com

Numbers displayed above are based on latest data collected.
For more information visit www.intechopen.com

Spinel Ferrite Nanoparticles: Correlation of Structure and Magnetism

Barbara Pacakova, Simona Kubickova,
Alice Reznickova, Daniel Niznansky and
Jana Vejpravova

Additional information is available at the end of the chapter

Abstract

This chapter focuses on the relationship between structural and magnetic properties of cubic spinel ferrite MFe_2O_4 (M = Mg, Mn, Fe, Co, Ni, Cu and Zn) nanoparticles (NPs). First, a brief overview of the preparation methods yielding well-developed NPs is given. Then, key parameters of magnetic NPs representing their structural and magnetic properties are summarized with link to the relevant methods of characterization. Peculiar features of magnetism in real systems of the NPs at atomic, single-particle, and mesoscopic level, respectively, are also discussed. Finally, the significant part of the chapter is devoted to the discussion of the structural and magnetic properties of the NPs in the context of the relevant preparation routes. Future outlooks in the field profiting from tailoring of the NP properties by doping or design of core-shell spinel-only particles are given.

Keywords: cubic spinel ferrite nanoparticles, magnetic properties, core-shell structure, particle size, spin canting, Mössbauer spectroscopy, magnetic susceptibility, size effect, superparamagnetism, magnetic anisotropy

1. Introduction

Spinel ferrite nanoparticles (NPs) are in the spotlight of current nanoscience due to immense application potential. Very interesting aspects of the spinel ferrite NPs are their excellent magnetic properties often accompanied with other functional properties, such as catalytic activity. Moreover, the magnetic response of the NPs can be tuned by particle size and shape

up to some extent. Consequently, various spinel ferrite NPs are suggested as universal and multifunctional materials for exploitation in biomedicine [1–4], magnetic recording, catalysis [5–8] including magnetically separable catalysts [9–12], sensing [13–16] and beyond ($MgFe_2O_4$ in Li ion batteries [17, 18], or investigation of dopamine [19]). Thus it is of ultimate interest to get control over their functional properties, which requires in-depth understanding of the correlation between their structural and magnetic order. For example, the particle size and shape are extremely important both in biomedical imaging using Magnetic Resonance Imaging (MRI) [20] and therapies by means of magnetic field-assisted hyperthermia [21].

The chapter aims to summarize the most important aspects of magnetism of cubic spinel ferrite nanoparticles (MFe_2O_4, M = Mg, Mn, Fe, Co, Ni, Cu, and Zn) in context of their crystal and magnetic structure. The factors that drive magnetic performance of the spinel ferrite NPs can be recognized on three levels: on the atomic level (degree of inversion and the presence of defects), at single-particle level as balance between the crystallographically and magnetically ordered fractions of the NP (single-domain and multi-domain NPs, core-shell structure, and beyond), and at mesoscopic level by means of mutual interparticle interactions and size distribution phenomena. All these effects are strongly linked to the preparation routes of the NPs. In general, each preparation method provides rather similar NPs by means of morphology and crystalline order. Thus the "three-level" concept, which is the focal motif of the chapter, can be applied to all cubic spinel ferrite NPs.

2. Brief overview of preparation methods of spinel ferrite nanoparticles

In this section, selected methods of the NP preparation are summarized. Explicitly, the wet methods yielding well-defined NPs, either isolated or embedded in a matrix, are accented. The reason is that only such samples can be sufficiently characterized and the factors defined within the "three level" concept can be disentangled. Outstanding reviews on the specific method(s) with further details and references are also included [22–25].

Coprecipitation method is the archetype route, which can be used for preparation of all cubic spinel ferrite NPs: Fe_3O_4/γ-Fe_2O_3 [24, 26], $MgFe_2O_4$ [27], etc. In general, two water-soluble metallic salts are coprecipitated by a base. The reaction can be partly controlled in order to improve characteristics of the NPs [26, 28, 29]; however, it is generally reported as a facile method yielding polydispersed NPs with lower crystallinity and consequently less significant magnetic properties.

The family of decomposition routes includes wet approaches based on decomposition of metal organic precursors in high-boiling solvents, typically in the presence of coating agents (all [30], Fe_3O_4/γ-Fe_2O_3 [24, 31], $CoFe_2O_4$ [32, 33], $NiFe_2O_4$ [34], $ZnFe_2O_4$ [35]). The most common organic complexes used for decomposition are metal oleates and acetylacetonates. The decomposition methods yield highly crystalline particles close to monodisperse limit with very good magnetic properties. However, the reaction conditions must be controlled in correspondence of the growth model suggested by Cheng et al. [22]. They can be also tailored to produce NPs of different shapes ($CoFe_2O_4$ [36, 37], Fe_3O_4/γ-Fe_2O_3 [38, 39]). Higher-order

assemblies of the NPs can be also achieved by varying the ratio of the precursor and reaction temperature ($CoFe_2O_4$ [40]). Alternatively, the decomposition takes place in high-pressure vessel (autoclave) [41, 42].

A large group of preparation protocols is based on solvothermal treatments, in aqueous conditions termed as hydrothermal. The preparation can be carried out either in a simple single-solvent system ($MgFe_2O_4$ [43], $NiFe_2O_4$ [44, 45]), mixture of solvents ($MnFe_2O_4$ [46], $ZnFe_2O_4$ [47]), surfactant-assisted routes ($ZnFe_2O_4$ [48]), or in multicomponent systems, such as water-alcohol-fatty acid ($Fe_3O_4/\gamma\text{-}Fe_2O_3$ [49], $CoFe_2O_4$ [50]). The solvothermal routes are often carried out at elevated pressure and can be also maintained in supercritical conditions ($MgFe_2O_4$ [51]). The NPs prepared by this class of methods are in general of very good crystallinity, in some cases competitive to the NPs obtained by the decomposition routes.

Spinel ferrite NPs can be also obtained with the help of normal or reverse micelle methods, often referred as microemulsion routes (all [52, 53], $Fe_3O_4/\gamma\text{-}Fe_2O_3$ [54], $MgFe_2O_4$ [55–57], $CoFe_2O_4$ [58], $NiFe_2O_4$ [59], $CoFe_2O_4$ and $MnFe_2O_4$ [60], $ZnFe_2O_4$ [61]). This approach takes advantage of the defined size of the micelle given by the ratio of the microemulsion components (water-organic phase-surfactant) according to the equilibrium phase diagram [62]. The micelles serve as nano-reactors, which exchange the constituents dissolved in the water phase during the reaction and self-limit the maximum size of the NPs. The as-prepared NPs are often subjected to thermal posttreatment, which improves the NP crystallinity and enhances magnetic properties. However, such NPs are no more dispersible in liquid phase and their applications are thus limited. On the other hand, the microemulsion technique can be used for preparation of the NPs of a defined shape [63] and mixed ferrites [64].

A modified polyol method is also used for preparation of spinel ferrite NPs [22, 24, 65–67]. While in the standard route the polyol acts as a solvent and sometimes reducing or complexing agent for metal ions, for preparation of the ferrite NPs, the reaction of 1,2-alkanediols and metal acetylacetonates in high-boiling solvents is the most common variant.

Sol-gel chemistry is a handy approach to produce spinel ferrite NPs. The common tactic is the growth of the NPs in porous silica matrix yielding well-developed NPs embedded in the transparent matrix. The route requires annealing of the gel; however, the particle size can be sufficiently varied by the annealing temperature. Different spinel ferrites can be prepared ($Fe_3O_4/\gamma\text{-}Fe_2O_3$ [68], $CoFe_2O_4$ [69–71], $MnFe_2O_4$ [72], $NiFe_2O_4$ [73–75]).

NPs of spinel ferrites are also prepared with assistance of microwaves [76, 77], ultrasound ($CoFe_2O_4$ [78], $MgFe_2O_4$ [79]), combustion routes ($MgFe_2O_4$ [80]), or mechanical treatments ($MgFe_2O_4$ [81], $MnFe_2O_4$ [82], $NiFe_2O_4$ [83]); however, the as-prepared NPs often require heat treatment, and the resulting samples with sufficient crystallinity are better classified as fine powders. Less common methods such as the use of electrochemical synthesis for the $\gamma\text{-}Fe_2O_3$ NPs [84] or $NiFe_2O_4$ [85] and synthesis employing ionic liquids for cubic magnetite NPs [86] were recently reported. NPs with size in the multicore limit were obtained by disaccharide-assisted seed growth [87]. Recently, combination of stop-flow lithography and coprecipitation was reported [88]. Typical TEM images of spinel ferrite NPs prepared by the most common routes are shown in **Figure 1**.
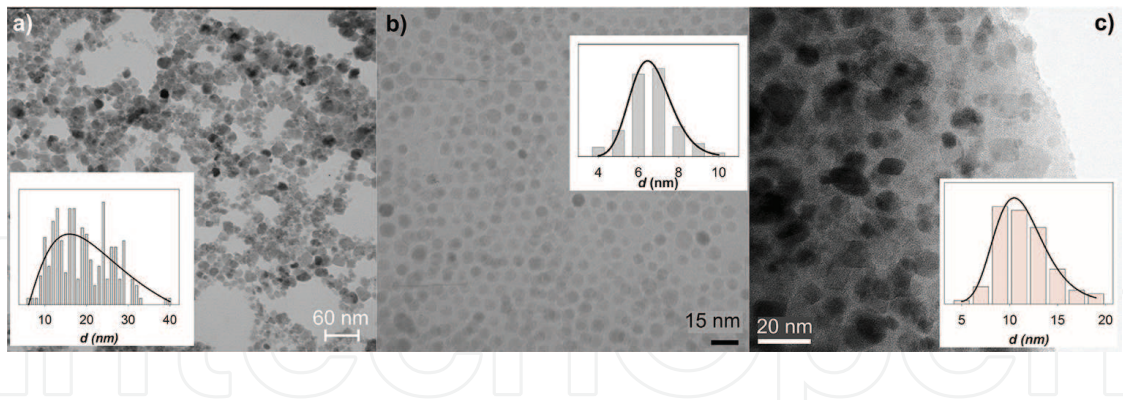
Figure 1. TEM images of the spinel NPs prepared by different methods, with distributions of particle diameters in the inset. (a) γ-Fe$_2$O$_3$ NPs prepared by coprecipitation technique. (b) CoFe$_2$O$_4$ NPs prepared by decomposition of oleic precursor. (c) ZnFe$_2$O$_4$ NPs prepared by sol-gel method.

The preparation methods described above can be successfully applied to preparation of core-shell NPs: CoFe$_2$O$_4$@MFe$_2$O$_4$; M = Ni, Cu, Zn or γ-Fe$_2$O$_3$ [89], and MnFe$_2$O$_4$@γ-Fe$_2$O$_3$ [90]; CoFe$_2$O$_4$@ZnFe$_2$O$_4$ [91]; CuFe$_2$O$_4$@MgFe$_2$O$_4$ [92]; or other mixed ferrites NPs [93, 94]. A natural core-shell structure is obtained for magnetite NPs due to topotactic oxidation to maghemite, which is mirrored, for example, in varying heating efficiency [95]. As a final remark, the selection of a particular preparation route yielding either a single core or multicore NPs is crucial and must be considered in the context of a specific application [96].

3. Characterization of magnetic nanoparticles: parameters and methods

In this section, the most important parameters characterizing structural and magnetic properties of NPs are introduced. Overview of the key experimental methods used for their evaluation is also included. For straightforwardness, details on the theoretical models and related formalism are not given, but relevant references are included. More details on the topic can be found in a comprehensive work by Koksharov [97].

3.1. Basic structural and magnetic characterization

The most important parameter is the particle size itself, usually attributed to the diameter of a single NP. The first-choice technique for determination of the particle size is the transmission electron microscopy (TEM), which gives the real (or physical) particle size, d_{TEM}. As the NPs of spinel ferrites are usually spherical, cubic, octahedral, or symmetric star-like objects, the value is a reasonable measure of the NP dimension as it gives information on the principal dimensions of those objects. Analysis of the TEM images also provides particle-size distribution, sometimes expressed as polydispersity index (PDI = $\sigma(d_{TEM})/\langle d_{TEM}\rangle$). The direct TEM observation gives information on aggregation, chaining of particles, and other morphological specifics. Using high-resolution TEM (HR TEM), internal structure of the NPs can be inspected, for example, the thickness of disordered surface layer and defects can be identified.

Particle size can be also determined using powder X-ray diffraction (XRD). The profile of the diffraction peak contains information about the so-called crystallite size, D_{hkl}, and the micro-strain (arise from the presence of vacancies, dislocation, stacking faults, or poor crystallinity of the material). Generally, the experimental profile is the convolution of the instrumental profile caused by the experimental setup and the physical profile caused by the intrinsic properties of the measured material [98].

The physical profile is the convolution of the two dominant contributions caused by the small D_{hkl} and by the microstrain. The D_{hkl} is defined as a coherently diffracting length in a crystallographic direction [hkl] that is parallel to the diffraction vector (surface normal) [98]. Assuming the spherical NPs with random orientation of individual [hkl] directions, the D_{hkl} determines the diameter of the coherently diffracting domain; in other words it is the diameter of the crystalline part of the NP, the d_{XRD}. For highly symmetric shapes expected for spinel ferrite NPs, the coherently diffracting domain can be sufficiently described by a sphere or an ellipsoid in the case of flat crystallites.

Other important parameters characterizing magnetic NPs are related to formation of a single-domain state. In order to decrease the magnetostatic energy that is associated with the dipolar fields, the ferromagnetic (or ferrimagnetic)-ordered crystal is divided into the magnetic domains. Within each of the domain, the magnetization, M reaches the saturation. The domain creation depends on the competition between the reduction of the magnetostatic energy and the energy required to form the domain walls separating the adjacent domains. The size of the domain wall is a balance between the exchange energy that tries to unwind the domain wall and the magnetocrystalline anisotropy with the opposite effect.

In the magnetic NPs, the typical dimensions are comparable with the thickness of the domain; thus, at some critical size, it is energetically favorable for the NP to become single domain. The critical dimension ranging from 10^{-7} to 10^{-8} m is strictly specific to each magnetic spinel ferrite [99].

In small magnetic NPs reaching the single-domain regime, the paramagnetic-like behavior can be observed even below the Curie temperature, T_c. The state is therefore called the superparamagnetism (SPM) as the whole particle behaves as one giant spin (superspin) consisting of the atomic magnetic moments; thus, the magnetic moment of the whole NP is 10^2 to 10^5 times larger than the atomic moment. The magnetization follows the behavior of the Langevin function. The theory of SPM and superspin relaxation of the NPs was treated by C. P. Bean, J.D. Livingston and M. Knobel. et al. [100, 101]. The key parameters representing the magnetic properties of single-domain NPs are blocking temperature, T_B, and superspin or NP magnetic moment, μ_m. The T_B is related to the particle size through its volume, V as:

$$T_B = K_{eff}V \: / \: (ak_B) \qquad (1)$$

where K_{eff} is the effective anisotropy constant. Parameter a is given by the measurement time, τ_m as $a = \ln(\tau_m / \tau_0)$, $a = 25$ for the SPM systems with relaxation time $\tau_0 = 10^{-12}$ s (see the following paragraphs) and $\tau_m = 100$ s [101, 102].

The μ_m is related to the saturation magnetization, M_s, which is defined as the maximum allowed magnetization at given temperature (all spins are aligned along the field direction) and often deviates from a theoretical bulk value. For ideal NPs (physical volume is identical with the volume where the magnetic structure is like in the bulk spinel), the dependence of μ_m on M_s can be written as $\mu_m = M_s V$.

Another important parameter is the relaxation time, τ of the NP superspin. For a particle with uniaxial anisotropy, the superspin relaxation corresponds to the flip between two equilibrium states separated by an energy barrier $K_{eff}V$, which can be overcome by the thermal fluctuations at the T_B. The superspin relaxation in the SPM systems is described by the Néel-Arrhenius law as [103, 104]:

$$\tau = \tau_0 \exp(E_A / k_B T) \tag{2}$$

where E_A is the anisotropy energy and other variables and constants have usual meaning.

Below the T_B, the NPs are in the so-called blocked state analogous to the ordered state (such as ferromagnetic or ferrimagnetic), and the magnetic moments are fixed into the direction of the easy axis and can only fluctuate around these directions. The T_B also depends on the time window of the measurements, τ_m. If the $\tau_m > \tau$, the NPs have enough time to fluctuate and the SPM state can be observed. On the other hand, if $\tau_m < \tau$, the blocked regime is observed. Thus, determination of the T_B is dependent on the used experimental technique (10^{-8} s for Mössbauer spectroscopy (MS), 1 s for magnetic measurements, $10–10^{-3}$ s for a.c. susceptibility measurements).

A very important parameter characterizing the blocked state is the coercivity, H_c (or coercive field) as it gives information on opening of the hysteresis loop. Depending on the dominant anisotropy term, the H_c value reaches values in fractions of $2K_{eff}/M_s$ [101, 105]. In general, the coercivity (and also remanence) of NPs with nonspherical shapes shows complex angular dependence due to the shape anisotropy [106]. In very small particles, the coercivity is an interplay between the surface disorder and surface anisotropy [107].

The typical magnetic measurements of the NP magnetic parameters yielding the above-described parameters can be summarized as follows: temperature dependence of the magnetization in low external applied field, the so-called zero field cooled curve (ZFC) and field cooled curve (FC); field dependence of the magnetization at fixed temperatures, the so-called magnetization isotherm (or hysteresis loop in the blocked state); and the a.c. susceptibility measurement. The ZFC-FC protocol reveals the value of the T_B, while the analysis of the magnetization isotherms in the SPM state serves for determination of the μ_m. From this value, the so-called magnetic size of a NP, d_{mag} (size of the magnetically ordered part), can be determined.

A unique tool used in characterization of spinel ferrite NPs is the Mössbauer spectroscopy. It is a dual probe both for structure and magnetism at local level based on recoilless resonant absorption of γ radiation. In general, information on coordination surroundings of the iron

cations, their valence, degree of inversion of the spinel structure, and orientation of spins on the cubic spinel sub-lattices can be obtained [108, 109].

The small spinel ferrite NPs exhibit relaxation time in order of 10^{-9} s that is close to the time window of the MS (10^{-8} s) allowing the study of relaxation of the NPs by means of MS [109, 110]. Furthermore, the big advantage of the MS is that it is not restricted to the well crystalline samples; thus, a non-well crystalline NP can be also investigated using MS. Finally, the so-called spin canting angle, usually attributed to the presence of the surface spins, can be estimated [111].

3.2. Real effects in magnetic nanoparticles

3.2.1. Size distribution

All real systems of the NPs exhibit an intrinsic size distribution, which must be considered in evaluation and interpretation of structural and magnetic data. The most common is the log-normal distribution (see **Figure 1**); however, Gaussian distribution has been also reported [112–114]. In the case of the TEM observation for the d_{TEM}, the NPs can be termed depending on the value of the PDI as monodisperse (PDI < 0.05–0.1), highly uniform (PDI < 0.2), and polydisperse (PDI > 0.2). Similar classification might be applied to the distribution of d_{XRD}; however, such in-depth analysis is usually not included in common Rietveld treatment of the XRD data. On the other hand, the role of size distribution by means of magnetic size, d_{mag}, and superspin values is extremely important for evaluation of magnetic properties. The mean magnetic moment per single NP, μ_m, and distribution width, σ, can be derived from the experimental data, $\mu_m = \mu_0 \exp(\sigma^2 / 2)$, as the magnetization as a function of the applied field, H, and temperature, T, in SPM state can be described as a weighted sum of Langevin functions [69, 115, 116]:

$$M(H,T) = \int_0^\infty \mu L\left(\frac{\mu H}{k_B T}\right) f_L(\mu)\,d\mu \tag{3}$$

where $L(x)$ represents the Langevin function and $f_L(\mu)$ is the log-normal distribution of magnetic moments μ. The NP size distribution also affects the character of ZFC and FC curves as it is mirrored in distribution of the T_B and K_{eff}, and suited models must be applied to obtain median values, T_{Bm} and distribution width σ as relevant parameters [117–120].

One of the possible approaches evaluating the T_B distribution is based on refinement of the ZFC temperature dependence of magnetization, $M_{ZFC}(T)$ which is given by equation [101, 121, 122]:

$$M_{ZFC}(T) \propto \frac{M_S^2 H}{3K_{eff}}\left[\frac{25}{t}\int t_B f(t_B)\,dt_B + \int f(t_B)\,dt_B\right] \tag{4}$$

where $t_B = T_B/T_{Bm}$ is the reduced blocking temperature of individual NPs and $f(t_B)$ is the log-normal distribution function of reduced blocking temperatures. The first term in Eq. (4) represents contribution of the NPs in the SPM state, whereas the second term belongs to the NPs in blocked state.

Typical examples of magnetization isotherms and ZFC-FC curves influenced by the particle-size distribution are shown in **Figure 2**, presenting unhysteretic magnetization isotherms (Langevin curves) for different values of μ and σ and ZFC-FC curves for different values of T_B and σ.
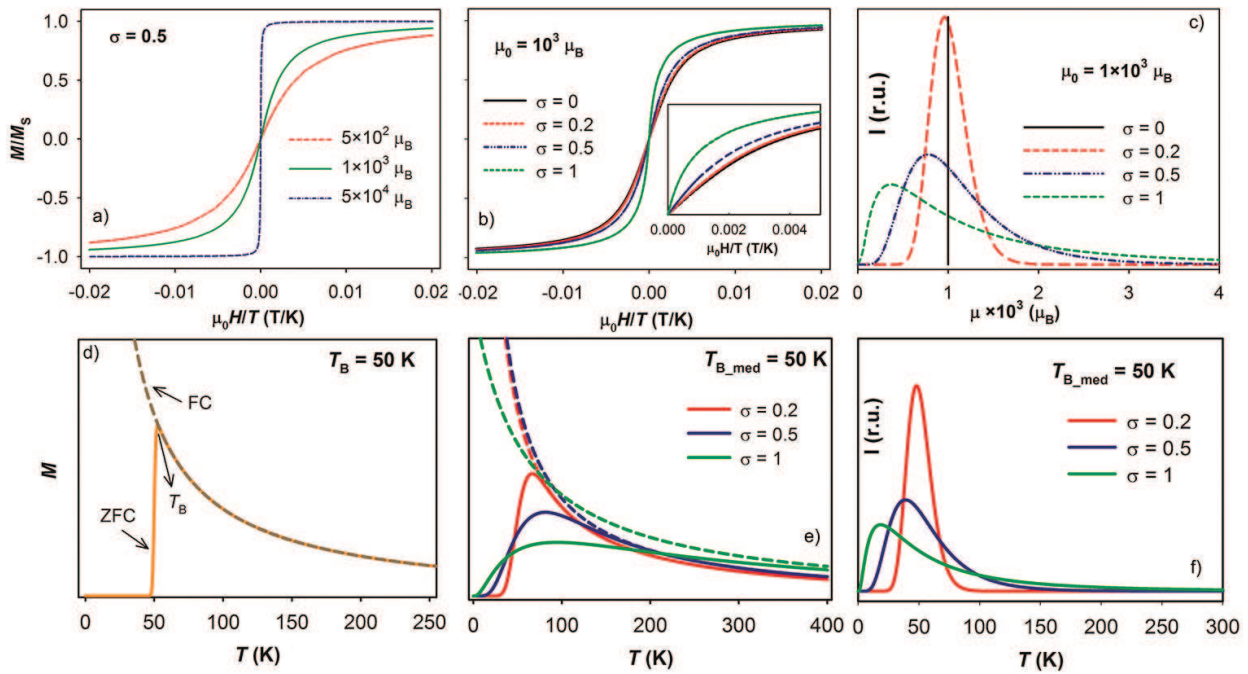

Figure 2. Model Langevin and ZFC-FC curves for selected NP magnetic moments and blocking temperature. (a) Langevin curves for magnetic moments with different orders of magnitude and $\sigma = 0.5$. (b) Evolution of Langevin curve for different magnetic moment distributions visualized in (c). (d) Ideal ZFC-FC curves for NP without size distribution. (e) Evolution of the ZFC-FC curve for fixed T_B and different distribution widths (f).

3.2.2. Spin canting phenomenon and surface effects

Decreasing the NP size, the number of atoms located at the surface dramatically increases. Thus the surface spins become dominant in the magnetic properties of the whole NP. The atoms at the surface exhibit lower coordination numbers originating from breaking of symmetry of the lattice at the surface.

Moreover, the exchange bonds are broken resulting in the spin disorder and frustration at the surface leading to the undesirable effects such as low saturation magnetization of the NP and the unsaturation of the magnetization in the high magnetic applied field [123]. To explain these effects, J. M. D. Coey proposed the so-called core-shell model in which the NP consists of a core with the normal spin arrangement and the disordered shell, where the spins are inclined

at random angles to the surface, the so-called spin canting angle [123] (see **Figure 3**). The spin canting angle in general depends on the number of the magnetic nearest neighbors connecting with the reduced symmetry and dangling bonds. Other effects such as the interparticle interactions play role [124]. The spin canting angle can be determined with the help of in-field Mössbauer spectroscopy (IFMS); an example is given in **Figure 4**.
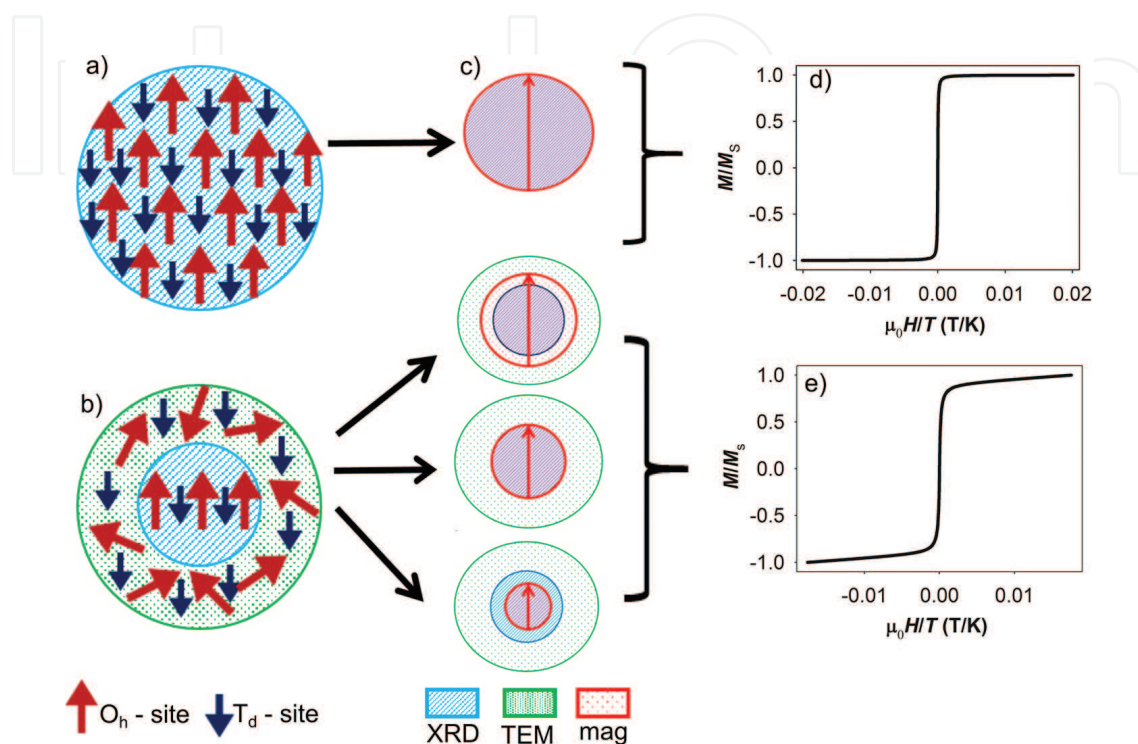

Figure 3. Scheme of the internal structure of ideal (a) and magnetic core-shell (b) structure of NP. (c) Scheme of the ideal and core-shell NP with the model of NP diameters determined by TEM, X-ray diffraction, and magnetic measurements. (d and e) Model Langevin curves for the ideal and core-shell NP with paramagnetic contribution due to the disordered spins in the NP shell.
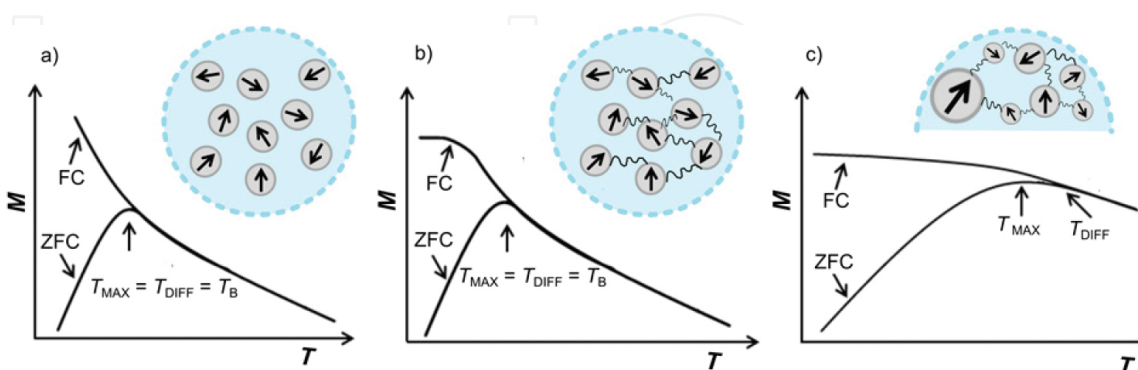

Figure 4. Schematic representation of the typical zero field cooled curve (ZFC) and field cooled curves (FC) for different types of NP ensembles. a) uniform NPs with negligible interparticle interactions, b) uniform NPs with "intermediate" interparticle interactions, c) NPs with non-negligible particle size distribution and strong interparticle interactions. The blocking temperature, T_B and the irreversibility temperature, T_{DIFF} typical for strongly interacting regime are shown.

However, the spin canting is not a unique property of the surface spins, and several works point to the volume nature of the effect [125–127]. Thus the surface effects in the NPs together with the origin of the spin canting angle are still discussed within the scientific community [109, 128–130].

Another consequence of the increased number of the surface atoms is the dominance of surface term to the anisotropy energy, usually expressed as a sum: $K_v + (6/d)K_s$, where K_v is the bulk value of the K_{eff} and K_s describes the contribution from the surface spins originated by structural deviations and spin frustration on the surface. Depending on the NP shape, the surface anisotropy may contain non-negligible admixture of higher-order Néel terms [130]. In real systems, the K_{eff} is additionally modified by the presence of other effects, mainly interparticle interactions described below.

3.2.3. Interparticle interactions

The interparticle interactions play a very important role in the magnetic response of the NPs, because they are usually not enough spatially separated to follow the behavior of an ideal SPM system. In general, two types of interaction can be observed: 1) the exchange interaction that affects mainly the surface spins of the NPs in close proximity thus can be neglected in most cases and 2) the long-range order dipolar interaction that is the dominant due to the high magnetic moment of the NPs [131].

The NP systems can be tentatively divided into the weakly interacting systems (the representatives are much diluted ferrofluids or NPs embedded in matrix in small concentration) and strongly interacting system with the powder samples as representatives. The strength of the interparticle interactions is given by the magnitude of the superspins and interparticle distance, in reality by the concentration of the NPs in ferrofluids, thickness of the NP coating, or matrix-to-NP ratio. The interparticle interactions affect all parameters characterizing the single-domain state. Furthermore, the strong interparticle interactions can result in the collective magnetic state at low temperature that resembles the typical physical properties of spin glasses [104], termed as superspin glasses in the case of strongly interacting SPM species [132–134].

In weakly interacting system, the dipolar interaction is treated as a perturbation to the SPM model within the Vogel-Fulcher law [104], the NP relaxation time is then written as:

$$\tau = \tau_0 \exp\left(E_A / k_B (T - T_0)\right). \tag{5}$$

The effect on the T_B is described by two models giving contradictory results on the relaxation times—the Hansen-Morup model (HM) [135] and the Dormann-Bessais-Fiorani model (DBF) [129]. The decrease of the T_B is predicted by the HM model, while its increase was obtained by the DBF model. So far, there have been no clear experimental evidences for a preference of one of these models. Some authors suggested that a phenomenological correction to the T_B in the weakly interacting systems could be used in the same way as it is done fore the relaxation time by adding the phenomenological constant T_0 to the T_B of the SPM system [102, 136, 137]. A

different approach treats weak interparticle interactions as additional magnetic field acting on a single NP, when correction to the external magnetic field, $(1-H/H_K)^a$ is added to Eq. (1) [101].

In the case of strong interactions, the collective state of the NP condensates below a characteristic temperature—the so-called glass-transition temperature, T_g—and the equation for the relaxation time is usually given by scaling law for critical spin dynamics [131, 132]:

$$\tau = \tau_0 \left(T_m / T_g - 1 \right)^{zv} \qquad (6)$$

where T_m is the temperature of the maximum at the a.c. susceptibility curve and zv is the dynamical critical component. However; strongly interacting systems do not necessarily fulfill criteria for the so-called superspin-glass systems obeying Eq. (6). Then, one of the approaches dealing with the effect of strong interactions on shift of the T_B is treated within the random anisotropy model (RAM) [101, 138–140]. RAM predicts the increase of interparticle interactions with decreasing correlation length, L which is a measure of average distance at which the magnetization fluctuations within the NP system are correlated. Then the K_{eff} and particle volume V are averaged to the number N of the NP involved in the interactions, introducing new K_L and V_L variables, and consequently, the formula for the T_B is modified to:

$$T_B = K_L V_L N^{1/2} \qquad (7)$$

The heart of the problem of calculating the T_B for interacting systems within the RAM model is the correct evaluation of the K_L and V_L of NP system.
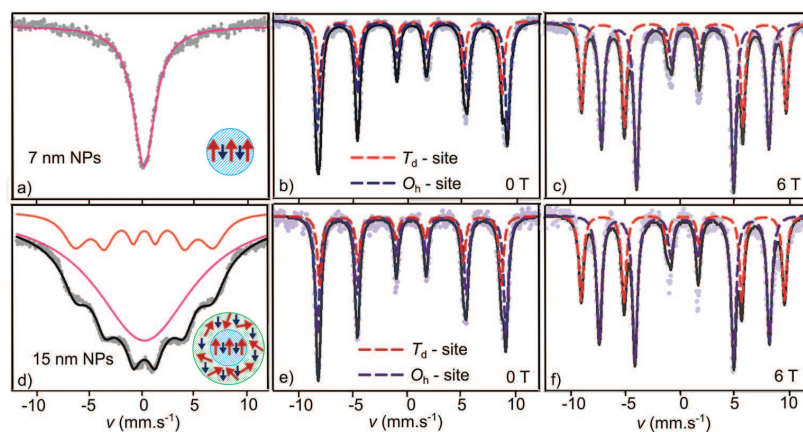

Figure 5. Typical MS spectra of almost ideal and core-shell NPs. The first column shows comparison of room-temperature MS spectra for the perfectly crystalline and ordered 7nm -Fe2O3 NPs (a) and core-shell 15 nm with 7 nm crystalline cores (d). The pink line is the fit of the spectra attributed to the fraction of NPs in SPM state. The middle and right column shows evolution of MS at low temperatures (4 K) in 0 T (b and e) and 6 T(c and f), respectively. Splitting of the lines attributed to the octahedral and tetrahedral positions can be disentangled after application of external magnetic field (c and f). Peak widening due to the disordered magnetic spins in the NP shell (d) is observable on the 4 K spectra (e and f), especially for the 1st and 6th lines.

The presence of interparticle interactions (as well as the particle-size distribution) is usually evidenced on the ZFC-FC curves; typical examples of medium and strongly interacting ensembles of NPs in comparison to the ideal noninteracting case are given in **Figure 5**. In real samples, all effects are present with variable contribution, and in some cases, both the size distribution and interparticle interactions must be addressed to describe the magnetic response of the samples properly [141, 142] (**Figure 5**).

4. Synergy of structural and magnetic probes

In order to provide complete insight into properties of magnetic NPs, synergy of structural and magnetic probes is essential. At the atomic and single-particle level, the complementarity of the (HR) TEM and XRD provides information on phase composition, the presence and type of defects, and particle sizes: d_{XRD} and d_{TEM}. The analysis of MS gives important knowledge on the degree of inversion and spin canting, which is then considered for interpretation of the magnetization data. Moreover, the particle-size distribution obtained from the TEM should be confronted with the superspin distribution obtained by the analysis of the Langevin curves; this analysis also yields the magnetic size, d_{mag}. Using the three different particle-size parameters (d_{mag}, d_{XRD}, d_{TEM}), the concept of the core-shell model of NP can be extended as the core-shell structure of the spins is often not identical with the crystallographically ordered-disordered part of the NP. The reason is that the spin frustration and disorder usually occur at volume larger than the size of the crystalline part. Comparing the d_{mag}, d_{XRD}, and d_{TEM} values, a very good estimate of the particle crystallinity and degree of spin order is obtained. A schematic representation of the crystallographic (structural) and magnetic core-shell model structures together with typical magnetization isotherms in the SPM state are shown in **Figure 3**.

At the mesoscopic level, the influence of interparticle interactions should not be neglected. For that purpose, morphology of the NP ensembles observed by the TEM gives estimate of mutual interparticle distance. The relevance of the interaction regime can be corroborated by a.c. susceptibility experiments, which yields characteristic relaxation times of the superspins, τ. As discussed above, those are strongly reformed because of the interactions. Finally, the effect of the μ, T_B, and K_{eff} distribution must be then carefully disentangled in order to estimate the pure contribution of the interaction.

5. Impact of preparation and strategies of tuning magnetic properties

The intrinsic NP parameters at all levels are imprinted during the preparation process. In this section, a brief discussion of this issue is given in the view of the "three-level" concept considering the structural and spin order in the unit cell and coordination polyhedra, single-particle, and NP ensemble level. Strategies profiting from the control over the imprint of the real effects by substitution or formation of artificial core-shell structures are also mentioned.

The degree of inversion, δ of the spinel structure is found to be significantly influenced by the preparation of the spinel ferrite NPs. In bulk, the normal or inverse spinel structure usually

dominates. However, the degree of inversion in the NPs is often close to 0.5 and the mixed spinel structure is the most common. For example, the $NiFe_2O_4$ is a typical inverse spinel, while in NPs obtained by the sol-gel method, the δ value of 0.6 was reported [143]. A very similar values were observed for sol-gel-prepared NPs of $CoFe_2O_4$ [69] (inverse spinel in bulk) and of $ZnFe_2O_4$ with normal spinel bulk structure [144]. The cation distribution in NPs prepared by coprecipitation method also often corresponds to mixed spinel structure as was demonstrated for $ZnFe_2O_4$ [145] and $MnFe_2O_4$ [146]. Moreover, the δ value can be controlled in the NPs prepared by the polyol method [65] and using tailored solvothermal protocols [147]. In addition, the stoichiometry of the NPs is not always matching the expected $M^{2+}/M^{3+}/O^{2-}$ ratio (1:2:4), e.g., as reported for NPs prepared by hydrothermal method [50].

The presence of defects, mainly by means of oxygen vacancies, is believed to be another important factor driving magnetic properties of the NPs. It was shown that they dominate the properties of the NPs obtained by mechanochemical processes [148], and it was also demonstrated that the level of defects can be influenced by vacuum annealing [149–151]. A specific issue is related to the presence of the Verwey transition in the Fe_3O_4 NPs [152] as the topotactic oxidation from magnetite to maghemite is a rapid process in common environments. Consequently, experimental investigations of the iron oxide NPs with size below 20 nm do not evidence the transition [26, 153]. Recently, the Verwey transition was observed in the NPs with a size of 6 nm, which were kept under inert atmosphere, and thus their oxidation was prevented [154].

The most significant and discussed issue is the spin order at single-particle level and its surface to volume nature. Most works report the dominance of surface spin frustration and suggest the presence of the magnetically dead layer. The increased contribution of the frustrated spins is attributed mainly to size effect, low crystallinity, and surface roughness, dominating in the NPs obtained by coprecipitation method [26, 155–165]. The spin canting in the surface layer was also observed in diluted ferrofluids, which confirms the nature of the effect on single-particle level [166]. However, the surface spin structure can be reformed when the NPs are in close proximity [131]. Significant increase of the amount of disordered spins was reported for hollow NPs of $NiFe_2O_4$ thanks to the additional inner surface [167]. On the other hand, the spin canting was also considered as volume effect, which occurs due to ion order-disorder in the spinel structure [127, 168] or pinning of the spins on internal defects in single NPs [125].

Focusing on the mesoscopic effects, the NP size distribution and interparticle interactions will be addressed. The particle-size distribution is found to be very sensitive to the preparation method used. The NPs with almost monodisperse character are obtained by the decomposition route; however, the parameters of the reaction must be carefully controlled. For example, the prolongation of the reaction time leads both to larger NPs but also increased size distribution [33, 169]. Similar effect was observed for increasing concentration of the oleic acid or oleylamine [33]. Other techniques provide NPs with PDI over 0.2, and the size distribution must be then considered in analysis of the magnetic measurements [69, 116, 142]. However, it is worth mentioning that the narrow-size distribution of the d_{TEM} does not automatically imply the same value of the d_{XRD} or d_{mag}, as shown, e.g., for maghemite NPs [125]. In majority of real samples, interparticle interactions contribute to the magnetic properties. In most cases, the samples are

studied in form of powders, which contain NPs in very close contact. Consequently, the response of such systems is always in the limit of the medium to strong interactions and is almost invariant to the preparation route used, and the interaction strength for a given NP size is given by minimum distance between the NPs, in other words by the thickness of the surface coating [42, 170–172]. Upon specific conditions, well-defined aggregates are formed [173], as reported, e.g., for preparations in microemulsion [174], by decomposition method [175] and by controlled encapsulation into phospholipides [176]. Such assemblies attracted interest due to considerably enhanced heating properties in hyperthermia [177], which is associated with the enhancement of the single-object (aggregate) anisotropy. In dense ensembles of the NPs, the onset of collective relaxation is also corroborated by significant increase of the relaxation time [178–184]; analogous consequence was observed in the aggregates [185]. However, the influence of the intra- and inter-aggregate interactions is not explicitly decoupled. Recent studies also suggest a strong influence of the reformed particle energy barrier on the details of the aging dynamics, memory behavior, and apparent superspin dimensionality of the particles [132].

In spite of the fact that the surface effects, defects, and interparticle interactions are believed to be contra-productive factors as they in general decrease the value of saturation magnetization [26], they were recognized as potential enhancers of effective magnetocrystalline anisotropy, reflected, for example, in increase of the hysteresis losses [186]. Consequently, attempts to prepare smart NPs based on artificial core-shell structure, e.g., $NiFe_2O_4@\gamma\text{-}Fe_2O_3$ [187], $ZnFe_2O_4@\gamma\text{-}Fe_2O_3$ [188], and $Co,Fe_2/Ni,Fe_2O_4$ [189], appeared recently. Tri-magnetic multi-shell structures prepared by high-temperature decomposition of the metal oleates were also reported [190].

Alternative strategy is the tuning of magnetic properties of the spinel ferrite NPs via site-specific occupation of the spinel lattice. This is a straightforward approach as the relevant metal ions can substitute each other in the spinel structure easily. In this case, however, the site occupation must be carefully evaluated and controlled. Successful preparation and basic investigation of structure and magnetic properties of the NPs of Mn-doped $CuFe_2O_4$ ferrite [191], Zn-doped $MnFe_2O_4$ [192] and $NiFe_2O_4$ [193, 194], Co-doped $NiFe_2O_4$ [195] and $ZnFe_2O_4$ [196], and Cr-doped $CoFe_2O_4$ [197] were reported. Recently, doping of spinel ferrites by large cations was suggested as a promising way to increase the effective magnetic anisotropy. La-doped $CoFe_2O_4$ [198], Sr-doped $MgFe_2O_4$ [199], and Ce-doped $NiFe_2O_4$ [200] or $ZnFe_2O_4$ [201] were prepared. For the doped samples, the most promising are the polyol, sol-gel, or microemulsion methods as they do not require identical decomposition temperatures of metal precursors like the organic-based routes, allow rather good control over homogeneity of doping, and yield samples with sufficiently low particle-size distribution.

6. Conclusions and outlooks

The core message of the chapter is to emphasize the importance of structural and spin order mirrored in magnetic properties of well-defined spinel ferrite nanoparticles (NPs). The

correlation between the specific preparation route to the typical structural and magnetic parameters of the particles is given, and the suitability of the resulting NPs in the context of possible applications is evaluated. Explicitly the meaning of different particle sizes obtained by different characterization methods, related to the degree of structural and spin order, is emphasized in the context of the magnetic properties. In order to wrap up the given subject, let's outline future outlooks in the field. The research of fine magnetic particles is progressively developing thanks to high demand on their practical exploitation, mainly in biomedicine. The forthcoming trend in customization of the magnetic NPs is obviously converging to control of the required magnetic properties at single-particle level by adjustment of the synthetic protocols, which lead to fine tuning of the particle size, shape, and degree of order [169, 202]. For example, enhancement of the specific absorption rate in NPs can be achieved in natural or arbitrary core-shell structures [203], via coupling of magnetically soft and hard ferrites for maximization of hysteresis losses [204] or by doping-driven enhancement of heat generation [205]. Finally, smart self-assembling strategies leading to superstructures [206], which can be even induced by magnetic field [207], seem to be a powerful tool for managing the magnetic response of the NPs at mesoscopic level.

Acknowledgements

Author details

Barbara Pacakova[1], Simona Kubickova[1], Alice Reznickova[1], Daniel Niznansky[2] and Jana Vejpravova[1,2*]

*Address all correspondence to: vejpravo@fzu.cz

1 Department of Magnetic Nanosystems, Institute of Physics of the Czech Academy of Sciences, Prague, Czech Republic

2 Department of Inorganic Chemistry, Faculty of Science, Charles University in Prague, Prague, Czech Republic

References

[1]   Bauer LM, Situ SF, Griswold MA, Samia ACS. Nanoscale 2016;8:12162–9. doi:10.1039/c6nr01877g.

[2]   Kanagesan S, Bin Ab Aziz S, Hashim M, Ismail I, Tamilselvan S, Alitheen NBBM, et al. Molecules 2016;21:312. doi:10.3390/molecules21030312.

[3]   Peng Y, Wang Z, Liu W, Zhang H, Zuo W, Tang H, et al. Dalt Trans 2015;44:12871–7. doi:10.1039/c5dt01585e.

[4]   Bae S, Lee SW, Takemura Y. Appl Phys Lett 2006;89:252503. doi:10.1063/1.2420769.

[5]   Ghahremanzadeh R, Rashid Z, Zarnani AH, Naeimi H. Appl Catal A Gen 2013;467:270–8. doi:10.1016/j.apcata.2013.07.029.

[6]   Zhang L, Wu Y. J Nanomater 2013;2013:640940–6. doi:10.1155/2013/640940.

[7]   Kumar AS, Thulasiram B, Laxmi SB, Rawat VS, Sreedhar B. Tetrahedron 2014;70:6059–67. doi:10.1016/j.tet.2014.01.051.

[8]   Pan L, Xu B. JOM 2013;65:695–701. doi:10.1007/s11837-013-0607-2.

[9]   El-Remaily MAEAAA, Abu-Dief AM. Tetrahedron 2015;71:2579–84. doi:10.1016/j.tet.2015.02.057.

[10] Tyrpekl V, Vejpravova JP, Roca AG, Murafa N, Szatmary L, Niznansky D. Appl Surf Sci 2011;257:4844–8. doi:10.1016/j.apsusc.2010.12.110.

[11] Tasca JE, Ponzinibbio A, Diaz G, Bravo RD, Lavat A, Gonzalez MG. Top Catal 2010;53:1087–90. doi:10.1007/s11244-010-9538-0.

[12] Wang ZL. RSC Adv 2015;5:5563–6. doi:10.1039/c4ra14486d.

[13] Ensafi AA, Allafchian AR, Mohammadzadeh R. Anal Sci 2012;28:705–10. doi:10.2116/analsci.28.705.

[14] Liu YL, Liu ZM, Yang Y, Yang HF, Shen GL, Yu RQ. Sens Actuat B Chem 2005;107:600–4. doi:10.1016/j.snb.2004.11.026.

[15] Vignesh RH, Sankar KV, Amaresh S, Lee YS, Selvan RK. Sens Actuat B Chem 2015;220:50–8. doi:10.1016/j.snb.2015.04.115.

[16] Sun Z, Liu L, Ha DZ, Pan W. Sens Actuat B Chem 2007;125:144–8. doi:10.1016/j.snb.2007.01.050.

[17] Pan Y, Zhang Y, Wei X, Yuan C, Yin J, Cao D, et al. Electrochim Acta 2013;109:89–94. doi:10.1016/j.electacta.2013.07.026.

[18] Zhang W, Hou X, Lin Z, Yao L, Wang X, Gao Y, et al. J Mater Sci Electron 2015;26:9535–45. doi:10.1007/s10854-015-3616-9.

[19] Reddy S, Swamy BEK, Chandra U, Mahathesha KR, Sathisha TV, Jayadevappa H. Anal Methods 2011;3:2792–6. doi:10.1039/c1ay05483j.

[20] Smolensky ED, Park HYE, Zhou Y, Rolla GA, Marjanska M, Botta M, et al. J Mater Chem B 2013;1:2818–28. doi:10.1039/c3tb00369h.

[21] Martinez-Boubeta C, Simeonidis K, Makridis A, Angelakeris M, Iglesias O, Guardia P, et al. Sci Rep 2013;3:1652. doi:10.1038/srep01652.

[22] Cheng K, Frey NA, Sun S, Peng S, Cheng K, Sun S. Chem Soc Rev 2009;38:2532–42. doi: 10.1039/b815548h.

[23] Salabas EL. Structural and Magnetic Investigations of Magnetic Nanoparticles and Core-Shell Colloids. Universität Duisburg-Essen, 2004. doi:http://purl.oclc.org/NET/duett-03182005-143720.

[24] Tartaj P, Morales M del PM, Veintemillas-Verdaguer S, González-Carreño T, Serna CJ. J Phys D Appl Phys 2009;42:224002. doi:10.1088/0022-3727/42/22/224002.

[25] Wu Z, Yang S, Wu W. Nanoscale 2016;8:1237–59. doi:10.1039/C5NR07681A.

[26] Roca AG, Niznansky D, Poltierova-Vejpravova J, Bittova B, Gonzalez-Fernandez MA, Serna CJ, et al. J Appl Phys 2009;105:114309. doi:10.1063/1.3133228.

[27] Chen Q, Rondinone AJ, Chakoumakos BC, Zhang ZJ. J Magn Magn Mater 1999;194:1–7. doi:10.1016/S0304-8853(98)00585-X.

[28] Roca AG, Morales MP, Serna CJ. IEEE Trans Magn 2006;42:3025–9. doi:10.1109/TMAG.2006.880111.

[29] Suppiah DD, Abd Hamid SB. J Magn Magn Mater 2016;414:204–8. doi:10.1016/j.jmmm.2016.04.072.

[30] Sun S, Zeng H, Robinson DB, Raoux S, Rice PM, Wang SX, Li G. J Am Chem Soc 2004;126:273–9. doi:10.1002/asia.201300068.

[31] Tartaj P, Morales MP, Veintemillas-Verdaguer S, Gonzales-Carre OT, Serna CJ. J Phys D Appl Phys 2003;36:R182–97. doi:10.1088/0022-3727/36/13/202.

[32] López-Ortega A, Lottini E, Fernández CDJ, Sangregorio C. Chem Mater 2015;27:4048–56. doi:10.1021/acs.chemmater.5b01034.

[33] Lu LT, Dung NT, Tung LD, Thanh CT, Quy OK, Chuc NV, et al. Nanoscale 2015;7:19596–610. doi:10.1039/c5nr04266f.

[34] Baruwati B, Manorama SV. Mater Chem Phys 2008;112:631–6. doi:10.1016/j.matchemphys.2008.06.018.

[35] Maiti D, Saha A, Devi PS. Phys Chem Chem Phys 2016;18:1439–50. doi:10.1039/c5cp05840f.

[36] Bao N, Shen L, An W, Padhan P, Turner CH, Gupta A. Chem Mater 2009;21:3458–68. doi:10.1021/cm901033m.

[37] Zhang K, Zuo W, Wang Z, Liu J, Li T, Wang B, et al. RSC Adv 2015;5:10632–40. doi: 10.1039/C4RA15675G.

[38] Guardia P, Labarta A, Batlle X. J Phys Chem C 2011;115:390–6. doi:10.1021/jp1084982.

[39] Liang WI, Zhang X, Bustillo K, Chiu CH, Wu WW, Xu J, et al. Chem Mater 2015;27:8146–52. doi:10.1021/acs.chemmater.5b03930.

[40] Cannas C, Ardu A, Peddis D, Sangregorio C, Piccaluga G, Musinu A. J Colloid Interface Sci 2010;343:415–22. doi:10.1016/j.jcis.2009.12.007.

[41] Douglas FJ, MacLaren DA, Murrie M. RSC Adv 2012;2:8027–35. doi:10.1039/c2ra20494k.

[42] Repko A, Vejpravova J, Vackova T, Zakutna D, Niznansky D. J Magn Magn Mater 2015;390:142–51. doi:10.1016/j.jmmm.2015.04.090.

[43] Nonkumwong J, Ananta S, Jantaratana P, Phumying S, Maensiri S, Srisombat L. J Magn Magn Mater 2015;381:226–34. doi:10.1016/j.jmmm.2015.01.001.

[44] Almeida TP, Fay M, Zhu Y, Brown PD. J Nanosci Nanotechnol 2012;12:8797–800. doi: 10.1166/jnn.2012.6467.

[45] Liu Q, Huang H, Lai L, Sun J, Shang T, Zhou Q, et al. J Mater Sci 2009;44:1187–91. doi: 10.1007/s10853-009-3268-3.

[46] Aslibeiki B, Kameli P, Ehsani MH, Salamati H, Muscas G, Agostinelli E, et al. J Magn Magn Mater 2016;399:236–44. doi:10.1016/j.jmmm.2015.09.081.

[47] Guo P, Cui L, Wang Y, Lv M, Wang B, Zhao XS. Langmuir 2013;29:8997–9003. doi: 10.1021/la401627x.

[48] Rameshbabu R, Ramesh R, Kanagesan S, Karthigeyan A, Ponnusamy S. J Supercond Nov Magn 2014;27:1499–502. doi:10.1007/s10948-013-2466-z.

[49] Repko A, Niznansky D, Matulkova I, Kalbac M, Vejpravova J. J Nanopart Res 2013;15. doi:10.1007/s11051-013-1767-2.

[50] Repko A, Niznansky D, Poltierova-Vejpravova J. J Nanopart Res 2011;13:5021–31. doi: 10.1007/s11051-011-0483-z.

[51] Sasaki T, Ohara S, Naka T, Vejpravova J, Sechovsky V, Umetsu M, et al. J Supercrit Fluids 2010;53:92–4. doi:10.1016/j.supflu.2009.11.005.

[52] Mathew DS, Juang RS. Chem Eng J 2007;129:51–65. doi:10.1016/j.cej.2006.11.001.

[53] Vestal CR, Zhang ZJ. Int J Nanotechnol 2004;1:240–63. doi:10.1504/IJNT.2004.003727.

[54] Makovec D, Kosak A, Znidarsic A, Drofenik M. J Magn Magn Mater 2005;289:32–5. doi: 10.1016/j.jmmm.2004.11.010.

[55] Holec P, Plocek J, Niznansky D, Vejpravova JP. J Sol-Gel Sci Technol 2009;51:301–5. doi: 10.1007/s10971-009-1962-x.

[56] Chandradass J, Jadhav AH, Kim H. Appl Surf Sci 2012;258:3315–20. doi:10.1016/j.apsusc.2011.11.092.

[57] Chandradass J, Kim KH. J Alloys Compd 2011;509:L59–62. doi:10.1016/j.jallcom.2010.10.090.

[58] Laokul P, Arthan S, Maensiri S, Swatsitang E. J Supercond Nov Magn 2015;28:2483–9. doi:10.1007/s10948-015-3068-8.

[59] Coskun M, Korkmaz M, Firat T, Jaffari GH, Shah SI. J Appl Phys 2010;107. doi: 10.1063/1.3359426.

[60] Vestal CR, Zhang ZJ. Nano Lett 2003;3:1739–43. doi:10.1021/nl034816k.

[61] Ahn Y, Choi EJ, Kim S, An DH, Kang KU, Lee BG, et al. J Korean Phys Soc 2002;41:123–8.

[62] Aubery C, Solans C, Prevost S, Gradzielski M, Sanchez-Dominguez M. Langmuir 2013;29:1779–89. doi:10.1021/la303817w.

[63] Nguyen TD. Nanoscale 2013;5:9455–82. doi:10.1039/c3nr01810e.

[64] Pemartin K, Solans C, Alvarez-Quintana J, Sanchez-Dominguez M. Colloids Surf A Physicochem Eng Asp 2014;451:161–71. doi:10.1016/j.colsurfa.2014.03.036.

[65] Ammar S, Jouini N, Fievet F, Stephan O, Marhic C, Richard M, et al. J Non Cryst Sol 2004;345:658–62. doi:10.1016/j.jnoncrysol.2004.08.162.

[66] Sui J, Zhang C, Li J, Cai W. J Nanosci Nanotechnol 2012;12:3867–72. doi:10.1166/jnn.2012.5872.

[67] Zhao H, Liu R, Zhang Q, Wang Q. Mater Res Bull 2016;75:172–7. doi:10.1016/j.materresbull.2015.11.052.

[68] Dormann JL, Viart N, Rehspringer JL, Ezzir A, Niznansky D. Hyperfine Interact 1998;112:89–92. doi:10.1023/A:1011088611227.

[69] Vejpravova J, Sechovsky V, Plocek J, Niznansky D, Hutlova A, Rehspringer JL. J Appl Phys 2005;97. doi:10.1063/1.1929849.

[70] Vejpravova J, Plocek J, Niznansky D, Hutlova A, Rehspringer JL, Sechovsky V. IEEE Trans Magn 2005;41:3469–71. doi:10.1109/TMAG.2005.854879.

[71] Hutlova A, Niznansky D, Rehspringer JL, Estournes C, Kurmoo M. Adv Mater 2003;15:1622. doi:10.1002/adma.200305305.

[72] Rivas P, Sagredo V, Rossi F, Pernechele C, Solzi M, Pena O. IEEE Trans Magn 2013;49:4568–71. doi:10.1109/TMAG.2013.2262039.

[73] Carta D, Loche D, Mountjoy G, Navarra G, Corrias A. J Phys Chem C 2008;112:15623–30. doi:10.1021/jp803982k.

[74] Chakraverty S, Mandal K, Mitra S, Chattopadhyay S, Kumar S. Jpn J Appl Phys Part I 2004;43:7782–7. doi:10.1143/JJAP.43.7782.

[75] Mitra S, Mandal K, Kumar PA. J Magn Magn Mater 2006;306:254–9. doi:10.1016/j.jmmm.2006.03.024.

[76] Phuruangrat A, Kuntalue B, Thongtem S, Thongtem T. Mater Lett 2016;167:65–8. doi:10.1016/j.matlet.2016.01.005.

[77] Galvao WS, Freire RM, Ribeiro TS, Vasconcelos IF, Costa LS, Freire VN, et al. J Nanopart Res 2014;16:2803–6. doi:10.1007/s11051-014-2803-6.

[78] Abbas M, Rao BP, Islam MN, Kim KW, Naga SM, Takahashi M, et al. Ceram Int 2014;40:3269–76. doi:10.1016/j.ceramint.2013.09.109.

[79] Barati MR, Selomulya C, Suzuki K. J Appl Phys 2014;115:17B522. doi:10.1063/1.4867751.

[80] Khot VM, Salunkhe AB, Thorat ND, Phadatare MR, Pawar SH. J Magn Magn Mater 2013;332:48–51. doi:10.1016/j.jmmm.2012.12.010.

[81] Pavlovic MB, Jovalekic C, Nikolic AS, Manojlovic D, Sojic N. Mater Sci Technol 2010;26:968–74. doi:10.1179/174328409X415020.

[82] Osmokrovic P, Jovalekic C, Manojlovic D, Pavlovic MB. J Optoelectron Adv Mater 2006;8:312–4.

[83] Zhou ZH, Xue JM, Wang J, Chan HSO, Yu T, Shen ZX. J Appl Phys 2002;91:6015–20. doi:10.1063/1.1462853.

[84] Starowicz M, Starowicz P, Zukrowski J, Przewoznik J, Lemanski A, Kapusta C, et al. J Nanopart Res 2011;13:7167–76. doi:10.1007/s11051-011-0631-5.

[85] Galindo R, Mazario E, Gutierrez S, Morales MP, Herrasti P. J Alloys Compd 2012;536:S241–4. doi:10.1016/j.jallcom.2011.12.061.

[86] Sundrarajan M, Ramalakshmi M. E J Chem 2012;9:1070–6. doi:10.1155/2012/541254.

[87] Tanaka T, Shimazu R, Nagai H, Tada M, Nakagawa T, Sandhu A, et al. J Magn Magn Mater 2009;321:1417–20. doi:10.1016/j.jmmm.2009.02.054.

[88] Suh SK, Yuet K, Hwang DK, Bong KW, Doyle PS, Hatton TA. J Am Chem Soc 2012;134:7337–43. doi:10.1021/ja209245v.

[89] Gomes JA, Azevedo GM, Depeyrot J, Mestnik-Filho J, Paula FLO, Tourinho FA, et al. J Phys Chem C 2012;116:24281–91. doi:10.1021/jp3055069.

[90] Goncalves ES, Cornejo DR, Oliveira CLP, Figueiredo Neto AM, Depeyrot J, Tourinho FA, et al. Phys Rev E 2015;91:42317. doi:10.1103/PhysRevE.91.042317.

[91] Masala O, Hoffman D, Sundaram N, Page K, Proffen T, Lawes G, et al. Sol State Sci 2006;8:1015–22. doi:10.1016/j.solidstatesciences.2006.04.014.

[92] Khedr MH, Bahgat M, El Rouby WMA. Mater Technol 2008;23:27–32. doi: 10.1179/175355508X266872.

[93] Morrison SA, Cahill CL, Carpenter EE, Calvin S, Harris VG. J Nanosci Nanotechnol 2005;5:1323–44. doi:10.1166/jnn.2005.303.

[94] Naik PP, Tangsali RB, Sonaye B, Sugur S. J Nano Res 2013;24:194–202. doi:10.4028/www.scientific.net/JNanoR.24.194.

[95] Lee SC, Fu CM, Chang FH. Appl Phys Lett 2013;103:163104. doi:10.1063/1.4825270.

[96] Gutiérrez L, Costo R, Grüttner C, Westphal F, Gehrke N, Heinke D, et al. Dalt Trans 2015:2943–52. doi:10.1039/c4dt03013c.

[97] Koksharov YA. Magnetic Nanoparticles, Wiley-VCH Verlag; 2009. p. 197–254.

[98] Rodriguez-Carvajal J, Roisnel T. In: Andersson, Y and Mittemeijer, EJ and Welzel U, editor. Eur Powder Diffr EPDIC 8, vol. 443–4, 2004, p. 123–6.

[99] Coey JMD. Magnetism and Magnetic Materials. 1st ed. New York: Cambridge University Press; 2009.

[100] Bean CP, Livingston JD. J Appl Phys 1959;30:S120–9. doi:http://dx.doi.org/10.1063/1.2185850.

[101] Knobel M, Nunes WC, Socolovsky LM, De Biasi E, Vargas JM, Denardin JC. J Nanosci Nanotechnol 2008;8:2836–57. doi:10.1166/jnn.2008.017.

[102] Singh V, Seehra MS, Bonevich J. J Appl Phys 2009;105:19–22. doi:10.1063/1.3073949.

[103] Dormann JL, Fiorani D, Cherkaoui R, Tronc E, Lucari F, Orazio FD, et al. J Magn Magn Mater 1999;203:23–7. doi:10.1016/S0304-8853(99)00180-8.

[104] Shtrikman S, Wohlfarth EP. Phys Lett 1981;85:467–70. doi:10.1016/0375-9601(81)90441-2.

[105] Cullity BD, Graham CD. Introduction to Magnetic Materials. New Jersey: John Wiley & Sons, Inc.; 2009.

[106] Corona RM, Altbir D, Escrig J. J Magn Magn Mater 2012;324:3824–8. doi:10.1016/j.jmmm.2012.06.022.

[107] Zhou CG, Schulthess TC, Landau DP. J Appl Phys 2006;99. doi:10.1063/1.2172557.

[108] Long GJ. Mössbauer Spectroscopy Applied to Inorganic Chemistry. 1st ed. New York: Plenum Publ. Corp.; 1984. doi:10.1007/978-1-4899-0462-1.

[109] Mørup S. Hyperfine Interact 1990;60:959–74. doi:10.1007/BF02399910.

[110] Gutlich P, Bill E, Trautwein AX. Mossbauer Spectroscopy and Transition Metal Chemistry: Fundamentals and Applications. 1st ed. Springer-Verlag Berlin Heidelberg; 2011. doi:10.1007/978-3-540-88428-6.

[111] Gonser U, Aubertin F, Stenger S, Fischer H, Smirnov G, Klingehoffer G. Hyperfine Interact 1991;67:701–9. doi:10.1007/BF02398222.

[112] Buhrman RA, Granqvist CG. Bull Am Phys Soc 1976;21:229.

[113] Granqvist CG, Buhrman RA. J Appl Phys 1976;47:2200–19. doi:10.1063/1.322870.

[114] Buhrman RA, Granqvist CG. J Appl Phys 1976;47:2220–2. doi:10.1063/1.322871.

[115] Fonseca FC, Goya GF, Jardim RF, Muccillo R, Carreño NLV, Longo E, et al. Phys Rev B 2002;66:104406. doi:10.1103/PhysRevB.66.104406.

[116] Ferrari E, da Silva F, Knobel M. Phys Rev B 1997;56:6086–93. doi:10.1103/PhysRevB.56.6086.

[117] Rondinone AJ, Samia ACS, Zhang ZJ. J Phys Chem B 1999;103:6876–80. doi:10.1021/jp9912307.

[118] Mamiya H, Ohnuma A, Nakatani I, Furubayashim T. IEEE Trans Magn 2005;41:3394–6. doi:10.1109/TMAG.2005.855205.

[119] Lee TH, Choi KY, Kim GH, Suh BJ, Jang ZH. Phys Rev B 2014;90:184411. doi:10.1103/PhysRevB.90.184411.

[120] Chowdhury D, Mookerj A. Phys B C 1984;124:255–8. doi:10.1016/0378-4363(84)90083-4.

[121] Hansen MF, Morup S. J Magn Magn Mater 1998;184:267–74. doi:10.1016/S0304-8853(97)01165-7.

[122] El-Hilo M, O'Grady K, Chantrell RW. J Magn Magn Mater 1992;114:295–306. doi:10.1016/0304-8853(92)90272-P.

[123] Coey JMD. Phys Rev Lett 1971;27:1970–2. doi:10.1103/PhysRevLett.27.1140.

[124] Tronc E, Fiorani D, Noguès M, Testa AM, Lucari F, D'Orazio F, et al. J Magn Magn Mater 2003;262:6–14. doi:10.1016/S0304-8853(03)00011-8.

[125] Kubickova S, Niznansky D, Morales MP, Salas G, Vejpravova J. Appl Phys Lett 2014;104:223105. doi:10.1063/1.4881331.

[126] Morrish AH, Haneda K. J Magn Magn Mater 1983;35:105–13. doi:10.1016/0304-8853(83)90468-7.

[127] Morales MP, Serna CJ, Bodker F, Morup S. J Phys Condens Matter 1997;9:5461–7. doi:10.1088/0953-8984/9/25/013.

[128] Mørup S, Brok E, Frandsen C. J Nanomater 2013;2013:720629. doi:10.1155/2013/720629.

[129] Dormann JL, Tronc E. In: Prigogine I, Rice SA, editors. Adv Chem Phys. Vol. 98. 1st ed., John Wiley & Sons, Inc., Hoboken, NJ, USA; 1997.

[130] Garanin DA, Kachkachi H. Phys Rev Lett 2003;90:65504. doi:10.1103/PhysRevLett. 90.065504.

[131] Mørup S, Hansen MF, Frandsen C. Beilstein J Nanotech 2010;1:182–90. doi:10.3762/ bjnano.1.22.

[132] Andersson MS, Angel De TJ, Lee SS, Normile PS, Nordblad P, Mathieu R Phys Rev B 2016;93:54407. doi:10.1103/PhysRevB.93.054407.

[133] Andersson MS, Mathieu R, Normile PS, Lee SS, Singh G, Nordblad P, et al. Mater Res Express 2016;3:45015. doi:10.1088/2053-1591/3/4/045015.

[134] Andersson MS, Mathieu R, Lee SS, Normile PS, Singh G, Nordblad P, et al. Nanotech-nology 2015;26:475703. doi:10.1088/0957-4484/26/47/475703.

[135] Hansen MF, Mørup S. J Magn Magn Mater 1998;184:262–74. doi:10.1016/ S0304-8853(97)01165-7.

[136] Seehra MS, Pisane KL. J Phys Chem Sol 2016;93:79–81. doi:10.1016/j.jpcs.2016.02.009.

[137] Pisane KL, Despeaux EC, Seehra MS. J Magn Magn Mater 2015;384:148–54. doi:10.1016/ j.jmmm.2015.02.038.

[138] Herzer G. NATO Sci Ser II Math Phys Chem 2003;184:15. doi:10.1007/1-4020-2965-9_2.

[139] Loffler J, Braun H, Wagner W. Phys Rev Lett 2000;85:1990–3. doi:10.1103/PhysRevLett. 85.1990.

[140] Luo W, Nagel SR, Rosenbaum TF, Rosensweig RE. Phys Rev Lett 1991;67:2721–4. doi.org/10.1103/PhysRevLett.67.2721

[141] Masunaga SH, Jardim RF, Correia MJ, Figueiredo W. J Phys Chem C 2016;120:765–70. doi:10.1021/acs.jpcc.5b10933.

[142] Pacakova B, Mantlikova A, Niznansky D, Kubickova S, Vejpravova J. J Phys Condens Matter 2016;28:206004–15. doi:10.1088/0953-8984/28/20/206004.

[143] Atif M, Nadeem M, Siddique M. Appl Phys A 2015;120:571–8. doi:10.1007/s00339-015-9216-y.

[144] Li FS, Wang L, Wang JB, Zhou QG, Zhou XZ, Kunkel HP, et al. J Magn Magn Mater 2004;268:332–9. doi:10.1016/S0304-8853(03)00544-4.

[145] Mozaffari M, Arani ME, Amighian J. J Magn Magn Mater 2010;322:3240–4. doi:10.1016/ j.jmmm.2010.05.053.

[146] Chinnasamy CN, Yang A, Yoon SD, Hsu K, Shultz MD, Carpenter EE, et al. J Appl Phys 2007;101:09M509. doi:10.1063/1.2710218.

[147] Vamvakidis K, Katsikini M, Sakellari D, Paloura EC, Kalogirou O, Dendrinou-Samara C. Dalt Trans 2014;43:12754–65. doi:10.1039/c4dt00162a.

[148] Goya GF, Rechenberg HR. J Magn Magn Mater 1999;196:191–2. doi:10.1016/S0304-8853(98)00723-9.

[149] Ayyappan S, Raja SP, Venkateswaran C, Philip J, Raj B. Appl Phys Lett 2010;96:143106. doi:10.1063/1.3374332.

[150] Ayyappan S, Paneerselvam G, Antony MP, Philip J. Mater Chem Phys 2011;128:400–4. doi:10.1016/j.matchemphys.2011.03.012.

[151] Philip J, Gnanaprakash G, Panneerselvam G, Antony MP, Jayakumar T, Raj B. J Appl Phys 2007;102:54305. doi:10.1063/1.2777168.

[152] Walz F. J Phys Condens Matter 2002;14:R285. doi:10.1088/0953-8984/14/12/203.

[153] Mitra A, Mohapatra J, Meena SS, Tomy C V, Aslam M. J Phys Chem C 2014;118:19356–62. doi:10.1021/jp501652e.

[154] Lee J, Kwon SG, Park JG, Hyeon T. Nano Lett 2015;15:4337–42. doi:10.1021/acs.nanolett.5b00331.

[155] Kodama RH, Berkowitz AE, McNiff EJ, Foner S. Phys Rev Lett 1996;77:394–7. doi:10.1103/PhysRevLett.77.394.

[156] Mitra S, Mandal K, Choi ES. IEEE Trans Magn 2008;44:2974–7. doi:10.1109/TMAG.2008.2002477.

[157] Nathani H, Gubbala S, Misra RDK. Mater Sci Eng B Sol State 2005;121:126–36. doi:10.1016/j.mseb.2005.03.016.

[158] Ahlawat A, Sathe VG, Reddy VR, Gupta A. J Magn Magn Mater 2011;323:2049–54. doi:10.1016/j.jmmm.2011.03.017.

[159] Oshtrakh MI, Ushakov MV, Senthilkumar B, Selvan RK, Sanjeeviraja C, Felner I, et al. Hyperfine Interact 2013;219:7–12. doi:10.1007/s10751-012-0660-1.

[160] Lestari KR, Yoo P, Kim DH, Liu C, Lee BW. J Korean Phys Soc 2015;66:651–5. doi:10.3938/jkps.66.651.

[161] Mendonca EC, Jesus CBR, Folly WSD, Meneses CT, Duque JGS. J Supercond Nov Magn 2013;26:2329–31. doi:10.1007/s10948-012-1426-3.

[162] Mendonca EC, Jesus CBR, Folly WSD, Meneses CT, Duque JGS, Coelho AA. J Appl Phys 2012;111:53917. doi:10.1063/1.3691792.

[163] Wang L, Zhou QG, Li FS. Phys Status Sol B 2004;241:377–82. doi:10.1002/pssb.200301923.

[164] Bakuzis AF, Morais PC, Pelegrini F. J Appl Phys 1999;85:7480–2. doi:10.1063/1.369383.

[165] Peddis D, Yaacoub N, Ferretti M, Martinelli A, Piccaluga G, Musinu A, et al. J Phys Condens Matter 2011;23:426004. doi:10.1088/0953-8984/23/42/426004.

[166] Sousa MH, Hasmonay E, Depeyrot J, Tourinho FA, Bacri JC, Dubois E, et al. J Magn Magn Mater 2002;242:572–4. doi:10.1016/S0304-8853(01)01122-2.

[167] Jaffari GH, Ceylan A, Ni C, Shah SI. J Appl Phys 2010;107:13910. doi:10.1063/1.3277041.

[168] Morales MP, Veintemillas-Verdaguer S, Montero MI, Serna CJ, Roig A, Casas L, et al. Chem Mater 1999;11:3058–64. doi:10.1021/cm991018f.

[169] Salas G, Casado C, Teran FJ, Miranda R, Serna CJ, Morales MP. J Mater Chem 2012;22:21065–75. doi:10.1039/C2JM34402E.

[170] Bullita S, Casu A, Casula MF, Concas G, Congiu F, Corrias A, et al. Phys Chem Chem Phys 2014;16:4843–52. doi:10.1039/c3cp54291b.

[171] Coskun M, Korkmaz M. J Nanopart Res 2014;16:2316. doi:10.1007/s11051-014-2316-3.

[172] Bittova B, Poltierova-Vejpravova J, Roca AG, Morales MP, Tyrpekl V. J Phys Conf Ser 2010;200:72012. doi:10.1088/1742-6596/200/7/072012.

[173] Vindedahl AM, Strehlau JH, Arnold WA, Penn RL. ES Nano 2016;3:494–505. doi:10.1039/C5EN00215J.

[174] Vejpravova JP, Tyrpekl V, Danis S, Niznansky D, Sechovsky V. J Magn Magn Mater 2010;322:1872–5. doi:10.1016/j.jmmm.2009.12.044.

[175] Peddis D, Cannas C, Musinu A, Piccaluga G. Chemistry 2009;15:7822–9. doi:10.1002/chem.200802513.

[176] Larsen BA, Haag MA, Serkova NJ, Shroyer KR, Stoldt CR. Nanotechnology 2008;19:265102. doi:10.1088/0957-4484/19/26/265102.

[177] Demortiere A, Panissod P, Pichon BP, Pourroy G, Guillon D, Donnio B, et al. Nanoscale 2011;3:225–32. doi:10.1039/c0nr00521e.

[178] Tackett RJ, Bhuiya AW, Botez CE. Nanotechnology 2009;20:445705. doi:10.1088/0957-4484/20/44/445705.

[179] Aslibeiki B, Kameli P, Salamati H. J Appl Phys 2016;119:63901. doi:10.1063/1.4941388.

[180] Aslibeiki B, Kameli P, Salamati H, Eshraghi M, Tahmasebi T. J Magn Magn Mater 2010;322:2929–34. doi:10.1016/j.jmmm.2010.05.007.

[181] Balaji G, Wilde G, Weissmuller J, Gajbhiye NS, Sankaranarayanan VK. Phys Status Sol B Basic Sol State Phys 2004;241:1589–92. doi:10.1002/pssb.200304671.

[182] Balaji G, Gajbhiye NS, Wilde G, Weissmuller J. J Magn Magn Mater 2002;242:617–20. doi:10.1016/S0304-8853(01)01043-5.

[183] Fannin PC, Vincent D, Massart G, Perov P, Neveu S. Eur Phys J Appl Phys 1999;8:247–51. doi:10.1051/epjap:1999252.

[184] Bittova B, Poltierova Vejpravova J, Morales MP, Roca AG, Mantlikova A. J Magn Magn Mater 2012;324:1182–8. doi:10.1016/j.jmmm.2011.11.005.

[185] Bittova B, Vejpravova JP, Morales MP, Roca AG, Niznansky D, Mantlikova A. Nano 2012;7:1250004. doi:10.1142/S179329201250004X.

[186] Vasilakaki M, Binns C, Trohidou KN. Nanoscale 2015;7:7753–62. doi:10.1039/c4nr07576e.

[187] Sousa EC, Rechenberg HR, Depeyrot J, Gomes JA, Aquino R, Tourinho FA, et al. J Appl Phys 2009;106:93901. doi:10.1063/1.3245326.

[188] Li J, Wang A, Lin Y, Liu X, Fu J, Lin L. J Magn Magn Mater 2013;330:96–100. doi:10.1016/j.jmmm.2012.10.048.

[189] Almeida TP, Moro F, Fay MW, Zhu Y, Brown PD. J Nanopart Res 2014;16:2395. doi:10.1007/s11051-014-2395-1.

[190] Gavrilov-Isaac V, Neveu S, Dupuis V, Taverna D, Gloter A, Cabuil V. Small 2015;11:2614–8. doi:10.1002/smll.201402845.

[191] Rai A, Banerjee M. J Nanosci Nanotechnol 2008;8:4172–5. doi:10.1166/jnn.2008.AN28.

[192] Beji Z, Hanini A, Smiri LS, Gavard J, Kacem K, Villain F, et al. Chem Mater 2010;22:5420–9. doi:10.1021/cm1001708.

[193] Jadhav SS, Shirsath SE, Toksha BG, Patange SM, Shengule DR, Jadhav KM. Phys B Condensed Matter 2010;405:2610–4. doi:10.1016/j.physb.2010.03.008.

[194] Kavas H, Baykal A, Toprak MS, Koeseoglu Y, Sertkol M, Aktas B. J Alloys Compd 2009;479:49–55. doi:10.1016/j.jallcom.2009.01.014.

[195] Kubickova S, Vejpravova J, Holec P, Niznansky D. J Magn Magn Mater 2013;334:102–6. doi:10.1016/j.jmmm.2013.01.005.

[196] Mehran E, Shayesteh SF, Nasehnia F. J Supercond Nov Magn 2016;29:1241–7. doi:10.1007/s10948-016-3415-4.

[197] Vestal CR, Zhang ZJ. Chem Mater 2002;14:3817–22. doi:10.1021/cm020112k.

[198] Burianova S, Vejpravova JP, Holec P, Plocek J, Niznansky D. J Appl Phys 2011;110:73902. doi:10.1063/1.3642992.

[199] Loganathan A, Kumar K. Appl Nanosci 2016;6:629–39. doi:10.1007/s13204-015-0480-0.

[200] Dixit G, Singh JP, Srivastava RC, Agrawal HM. J Magn Magn Mater 2013;345:65–71. doi:10.1016/j.jmmm.2013.05.060.

[201] Kuai S, Nan Z. J Alloys Compd 2014;602:228–34. doi:10.1016/j.jallcom.2014.03.049.

[202] Moya C, Morales MDP, Batlle X, Labarta A. Phys Chem Chem Phys 2015;17:13143–9. doi:10.1039/C5CP01052G.

[203] Phadatare MR, Meshram JV, Gurav KV, Kim JH, Pawar SH. J Phys D Appl Phys 2016;49:95004. doi:10.1088/0022-3727/49/9/095004.

[204] Zhang Q, Castellanos-Rubio I, Munshi R, Orue I, Pelaz B, Gries KI, et al. Chem Mater 2015;27:7380–7. doi:10.1021/acs.chemmater.5b03261.

[205] Mameli V, Musinu A, Ardu A, Ennas G, Peddis D, Niznansky D, et al. Nanoscale 2016;8:10124–37. doi:10.1039/C6NR01303A.

[206] Singh G, Chan H, Baskin A, Gelman E, Repnin N, Kral P, et al. Science (80-) 2014;345:1149–53. doi:10.1126/science.1254132.

[207] Singh G, Chan H, Udayabhaskararao T, Gelman E, Peddis D, Baskin A, et al. Faraday Discuss 2015;181:403–21. doi:10.1039/c4fd00265b.